P1.23

INVERSION-LAYER BREAKUP IN STEEP VALLEYS AND THE EFFECTS OF TOPOGRAPHIC SHADING

Augustin G. Colette*, Robert L. Street
Stanford University, Stanford, California

1.INTRODUCTION

A deep understanding of the formation and breakup of stable layers in valleys is needed for prediction of the transport and mixing of pollution over a complex terrain. Under conditions of weak synoptic forcing, the surface cooling leads to the formation of an inversion layer whose stability inhibits the vertical mixing. Over a flat terrain, the solar heating of surface in the morning induces the destruction of this stable layer by creating a convective boundary layer. In steep valleys, the nighttime down-slope and daytime up-slope winds should not be neglected when studying inversion layer formation and breakup. This phenomenon has been reported by a number of field studies (Whiteman 1990, Brehm and Freytag 1982 and Sakiyama 1990) and it has been reproduced in numerical simulations, e.g., by Anquetin *et al*. (1998).

Numerical simulations in idealized valleys are particularly interesting since it allows one to study how the inversion breakup is affected by the topography-related winds without modifying any of the other factors. To achieve this, the Advanced Regional Prediction System (A.R.P.S.), an operational, three-dimensional, compressible and non-hydrostatic modeling tool developed by the Center for Analysis and Prediction of Storms was chosen.

2.MODEL SETUP

A.R.P.S. is extensively described in Xue *et al.* (1995); this section summarizes the main parameters used in the simulation of valley flows.

2.1. *Numerical Parameters*

The momentum and scalar advection terms are solved using a fourth-order horizontal and second-order vertical differencing scheme and a leapfrog scheme with a $2s$ timestep. The active accoustic waves are solved separately with a $0.3s$ timestep. The subgrid scale turbulent mixing model is the 1.5 turbulent kinetic energy isotropic model of Deardorff and Moeng. The Coriolis force is neglected due to the small size of the domain and moist processes are activated to limit the range of temperatures observed in dry simulations.

The grid size ranges from $nx \times ny \times nz = 67 \times 18 \times 40$ to $101 \times 18 \times 40$, depending on the width of the valley simulated. The horizontal resolution is $200m \times 200m$ and a stretching is applied on the vertical grid from $30m$ to $150m$.

The east and west lateral boundary conditions are periodic, while the north and south boundaries are open radiative. Together with the idealized topography used in the simulations, these conditions impose a perfectly two–dimensionnal flow in the east-west planes. The top boundary condition is linear hydrostatic radiation with a Rayleigh damping layer at the top third of the domain.

The simulations presented hereafter are perfomed on Compaq/Alpha 667 MHz CPUs on which the computational to simulated time ratio is approximately 1.

*Corresponding author address: Environmental Fluid Mechanics Laboratory, Stanford, CA 94305-4020, (650) 723-1825, augustin@stanford.edu.

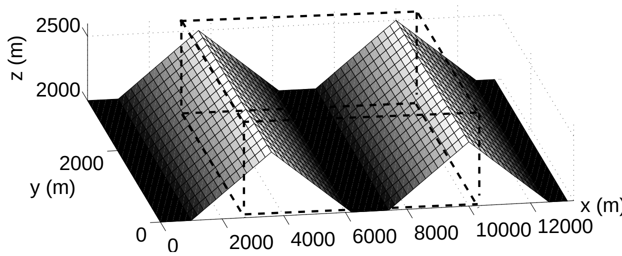

Figure 1: Topography used in the simulations of inversion breakup in idealized valleys with $H = 500m$ and $W = 1200m$.

2.2 *Physical Parameters*

The destruction of the inversion layer is investigated in several three dimensional valleys. Most previous numerical studies consider only a valley located between two ridges (Bader and McKee 1983, McNider and Pielke 1984 and Anquetin *et al*. 1998); however we found that a topography similar to that of de Wekker *et al*. (1998) in the study of plain to basin flows is needed to account for the convergence of up-slope winds above the ridges. Consequently, the basic topography consists of two triangular hills located on the sides of a flat valley (see figure 1). The size of the valley floor at the east and west boundaries must be chosen carefully so that the topography is periodic in the east-west direction, otherwise, as described by Hennemuth (1985), an energy casade from the small to the large valleys will occur.

The floor of the valley is horizontal, thus the along valley component of the wind will not be discussed. Kuwagata and Kimuro (1995) and Whiteman (1990) observed that before noon, the cross valley circulation prevails compared to the along valley winds, suggesting that the inversion breakup would be well reproduced in a flat-bottomed valley.

Several simulations have been performed with various widths of the valley floor (W) and ridge heights (H), while the half-width of the ridges remains constant at $2600m$. Before its use in A.R.P.S., this terrain is processed using a 4-pass Barnes Scheme to smooth its sharp edges (see A.R.P.S. 4.0 User's Guide 1995).

As several field studies have been conducted in either the Rocky Mountains, Japan or the Alps, this theoretical topography is located at $40^\circ N$ of latitude and $0^\circ E$ of longitude so that the local and UTC time are equal. Moreover, for better comparison with elevated valleys, its bottom lies at $2000m$ asl.

The soil type is chosen to be loam, and vegetation cover is grassland with shrubs. These surface characteristics are uniform over the valley and chosen so that the modeled valley is a typical Colorado valley. A bulk average was done between the Eagle, the Yampa and the Brush Creek valleys caracteristics (see Whiteman 1982 and Clements *et al*. 1989). As described in Xue *et al*. (2001), the soil data are extracted from the State Soil Geographic data base, the vegetation and the roughness length ($0.07m$) are diagnosed from the world ecosystem classes. The Normalized Difference Vegetation Index, is used to compute the leaf area index (0.2) and the vegetation fraction (0.5).

The surface and deep soil moisture are mainly used as tuning parameters. The deep soil is relatively dry (saturation rate of 0.05) so that the warming of the surface is fast enough in the morning and the surface soil is wet (saturation rate of 0.3) to avoid too much cooling at night.

All the simulations take place September 1st. The initialization occurs at 05:00Z, when the atmosphere is slightly stable all over the domain to avoid any vertical forcing. The potential temperature is started at $296K$ near the ground and the atmosphere is stratified with a buoyancy frequency $N = 0.019s^{-1}$. The initial surface temperature is that of the first layer of air, while the deep ground is $15K$ warmer to account for its thermostat role. A slight westerly wind of $0.1m/s$ is added to the inital base state to prevent excessive cooling at the beginning of the simulation. To avoid dependancy on the initial base state, only the second day simulated is analyzed.

3.VALLEY WINDS AND INVERSION BREAKUP IN IDEALIZED VALLEYS

3.1. *Inversion Breakup in a Steep Valley*

Figure 2 represents four slices in the east-west direction taken in the center of the domain. On these plots, both the wind vectors and the stability class are plotted. The stability of the atmosphere is diagnosed from the potential temperature averaged in the north-south direction using the Pasquill-Gifford classification (see table 1).

Stability class	Potential temperature gradient (° C /100m)
6 extremely unstable	< -0.9
5 moderately unstable	-0.9 to -0.7
4 slightly unstable	-0.7 to -0.5
3 neutral	-0.5 to 0.5
2 slightly stable	0.5 to 2.5
1 moderately stable	> 2.5

Table 1: Relationship between Pasquill-Gifford stability class and potential temperature stratification (adapted from Seinfeld and Pandis (1997)).

The first slice is taken in the early morning, at 08:00Z after the sun rose at 05:30Z on the east facing slope. The day before, a convective layer developed over the first $1.5km$ while the atmosphere remained slighlty stable above. At night, a shallow inversion layer ($100m$ deep) formed in the center of the valley and the stable part of the atmosphere extends up to $600m$. Due to the relatively large volume of the valley compared with shallower cases, the stratification did not become very strong in the valley, especially along the slopes. At 08:00Z, the winds are very weak in the valley even if an up-slope flow develops on the east facing slope.

At 09:00Z, the situation changed dramatically. While the up-slope winds develop on the east facing slope, an unstable layer appears and the inversion is destroyed. A deep stable core remains in the center of the valley and is weakened by both the growth of the convective boundary layer and the sinking of air induced by the removal of mass in the bottom of the valley by the slope winds.

By 10:00Z, the up-slope winds are well-developed on both slopes even though they are stronger on the east face. The stable layer is completely destroyed and most of the atmosphere is neutral in the valley. An unstable layer developed along the east-facing slope and before noon, it will extend to the other side.

In the evening, a couple of hours after sunset (20:00Z), the down-slope winds flow back toward the valley while a stable layer develops above the floor.

Most of the main characteristics of inversion breakup in steep valleys are reproduced in these idealized cases; the order of magnitude of the up- and down-slope winds, the depth of the stable layer and most importantly the destruction of the stable layer by an adiabatic warming of sinking air are in good agreement with field studies (see Whiteman 1982, Brehm and Freytag 1982 and Sakiyama 1990).

3.2. *Inversion Breakup in Various Valleys*

This simulation has been performed for six valleys of varying depth ($100m$, $500m$ and $1500m$) and floor width ($1200m$ and $4800m$) and above a flat terrain. The same setup has been used for all the simulations so that we can diagnose the influence of the topography on the inversion breakup.

Over a flat terrain the inversion and stable layers develop on the first $150m$ and $200m$ respectively. The breakup of the inversion begins at 08:00Z and is completed by 10:00Z, it is only driven by the growth of a convective boundary layer following the pattern 1 described in Whiteman (1982), the top of the stable layer remains constant during the breakup.

It is particularly interesting to compare this breakup with that over a deep valley. Figure 3 represents the time series of the vertical extent of the inversion and stable layer averaged in the north-south direction and across the valley floor. From this we conclude:

1. *Inversion and stable layers depth*: The depth of the stable layer increases with the height of the ridges. This has been reported by numerous field studies. However, due to the increasing volume of the valley, the inversion becomes more shallow when H increases. If the air cools enough to create a deep stable layer, this cooling is not sufficient to build an inversion.
2. *Lifetime of the inversion and stable layers*: As a consequence of the decrease of the inversion depth with H, its lifetime is much smaller in the deepest valleys. Concerning the stable layer, even if its depth increases, its lifetime remains approximately constant while the depth of the valley increases. Moreover, the breakup of the stable layer is faster in the narrow

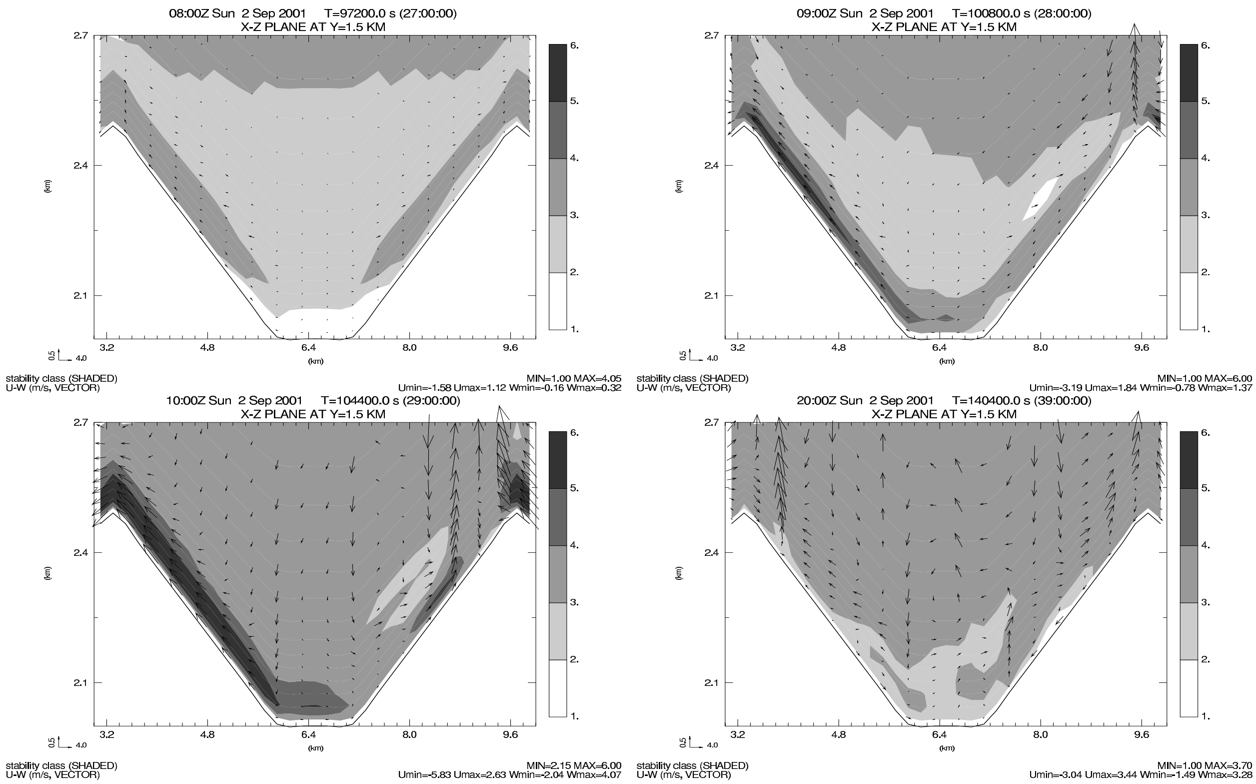

Figure 2: Evolution of the wind field (vectors) and stability class (filled isocontour) in an idealized valley ($W = 1200m$ and $H = 500m$) at 08:00Z, 09:00Z, 10:00Z and 20:00Z.

valleys. This feature corroborates the fact that the slope winds enhance the inversion breakup.

3. *Stable layer breakup pattern*: The only pattern we observe in these valleys is Whiteman's Pattern 3. Nevertheless, there are some differences between the simulated patterns. When the width of the valley decreases, the influence of the adiabatic warming of sinking air is stronger so that the stable layer is destroyed more from its top than in the wide case where, comparatively, it is closer to the pattern of the breakup over flat terrain. The cross-section of the wind field in the wide valleys shows that the floor is large enough to let convective cells grow, so that the stable layer is destroyed from the bottom. In the narrow case, the descent of air begins earlier in the deep valleys causing the lifetime of the stable layer to be similar to that of the shallow valley.

To summarize, these simulations point out the importance of the slope winds on the inversion breakup. The removal of mass in the bottom of the valley and the consequent sinking and warming of air seems to be a major factor of the breakup of the stable layer.

4. TOPOGRAPHY INDUCED SHADE

4.1. *Method*

A.R.P.S. 5.0 Beta 5 accounts for the angle between the slope and the sun rays so that the north face is not illuminated if the sun is at the south. Consequently the asymmetry between the east and the west facing slopes

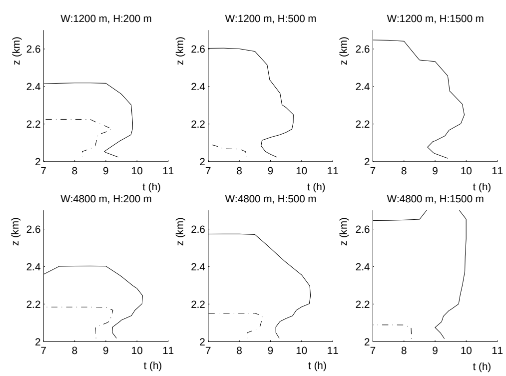

Figure 3: Time series of the vertical extent of the inversion (dashdotted line) and stable (solid line) layers in six valleys of varying depth (H) and width (W).

is well reproduced as we saw in the previous section. However, considering that the topographic shadow can delay the sunrise up to several hours (Whiteman 1982), we decided to take into account of the topographic shade in our model.

To diagnose if a grid point is illuminated or not, we draw a line between each surface node and the sun to check if this lines hits the topography. Considering that this shading will be useful only if the topography is highly resolved, the test is performed only on the grid cell boundaries. The radiation balance is then modified so that, at a shaded

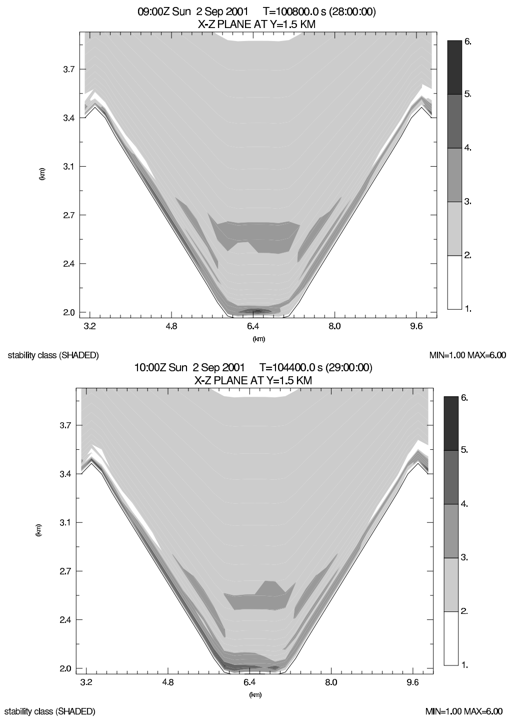

Figure 4: Vertical slice of the stability class. Top: at 09:00Z without taking into account of the topographic shade, bottom: at 10:00Z with topographic shading.

grid point, the incoming short wave solar radiation is set to zero.

4.2. ***Influence on the inversion breakup***

A test has been performed in a deep valley to analyze the influence of the topographic shade on the inversion breakup.

Figure 4 represents two slices of the atmospheric stability in the cross valley direction: at 09:00Z without shading (top) and at 10:00Z with shading (bottom). These two plots are very similar, showing that that the topographic shade delays the inversion break up approximately one hour. Moreover, the unstable strip near the surface exhibits less asymmetry in the non-shaded case.

The local sunrise in the center of the valley is 05:40Z for the non-shaded case and 07:50Z if we take into account the topographic shade. The discrepancy between the delay of the sunrise and that of the inversion breakup is due to the fact that in the second case even if the valley floor is shaded before 07:50Z, the slope is lit and consequently, up-slope winds begin to grow and to affect the inversion layer.

5. CONCLUSIONS

The breakup of the inversion layer in deep valleys is investigated using the Advanced Regional Prediction System. The slope winds and the characteristics of the stable layer are coherent with existing field study. Simulations in valleys of varying depth and width show that, in the steepest cases its destruction is mainly driven by the sinking of air induced by the removal of mass in the bottom of the valley due to the the up-slope winds.

The need of taking into account the topographic shade is underlined as it induces a delay in the inversion breakup of order one hour while the whole phenomenon lasts approximately two hours. This new subroutine will be most useful in simulation over a complex terrain where delay between the theoretical and local sunrises can reach several hours.

6. ACKNOWLEDGEMENTS

The support of AC by TotalFinaElf and RS by the DoE, Atm. Sci. Prog. of OBER and the Physical Meteorology Program of NSF is gratefully acknowledged.

7. REFERENCES

Anquetin, S., Guilbaud, C., and Chollet, J.-P., 1998: The formation and destruction of inversion layers within a deep valley. *J. Appl. Meteor.*, **37**, 1547-1560.

Bader, D.C. and McKee, T.B., 1983: Dynamical model simulation of the morning boundary layer development in deep mountain Valleys. *J. Appl. Meteor.*, **22**, 341-351.

Brehm, M. and Freytag, C., 1982: Erosion of the night-time thermal circulation in an alpine valley *Arch. Met. Geoph. Biokl.*, **B,31**, 331-352.

Clements, W.E., Archuleta, J.A. and Gudiksen, P.H., 1989: Experimental design of the ASCOT field study. *J. Appl. Meteor.*, **28**, 405-413.

DE Wekker, S.F.J., Zhong, S., Fast, J.D. and Whiteman, C.D., 1998: A numerical study of the thermally driven plain-to-basin wind over idealized basin topographies. *J. Appl. Meteor.*, **37**, 606-622.

Hennemuth, B., 1985: Temperature field and energy budget of a small alpine valley. *Beitr. Phys. Atmosph.*, **58**, 545-559.

Kuwagata, T. and Kimuro, F., 1995: Daytime Boundary Layer Evolution in a Deep Valley. Part 1: Observations in the Ina Valley. *J. Appl. Meteor.*, **34**, 1082-1091.

McNider, R.T. and Pielke, R.A., 1984: Numerical simulation of slope and mountain flows. *J. Appl. Meteor.*, **23**, 1441-1453.

Seinfeld, J. H. and Pandis, S. N., 1997: Atmospheric chemistry and physics : From air pollution to climate change. *John Wiley, New York.*, 1326p..

Sakiyama, S.K.,1990: Drainage flow characteristics and inversion breakup in two Alberta mountain valleys. *J. Appl. Meteor.*, **29**, 1015-1030.

Xue, M., Droegemeier, K.K., Wong, V., Shapiro, A. and Brewster, K., 1995: A.R.P.S. Version 4.0 User's Guide. *Center for Analysis and Prediction of Storms*, 380 p..

Xue, M., Droegemeier, K.K., Wong, V., Shapiro, A., Brewster, K., Carr, F., Weber, D., Liu, Y. and Wang, D.-H., 2001: The Advanced Regional Prediction System (A.R.P.S.) - A multiscale nonhydrostatic atmospheric simulation and prediction tool. Part II: Model physics and applications. *Meteorol. Atmos. Physics.*, **76**, 134-165.

Whiteman, C. D., 1982: Breakup of temperature inversions in deep mountain valleys. Part I: Observations. *J. Appl. Meteor.*, **21**, 270-289.

Whiteman, C. D., 1990: Observations of thermally developed wind systems in mountainous terrain. *In* Atmopsheric Processes Over Complex Terrain. *Meteor. Monogr.*, **45**, Amer. Met. Soc., 5-42.